J. Membrane Biol. 75, 129–139 (1983)

The Journal of
Membrane Biology

Impedance of the Electrogenic Cl^- Pump in *Acetabularia*: Electrical Frequency Entrainements, Voltage-Sensitivity, and Reaction Kinetic Interpretation

Jörg Tittor, Ulf-Peter Hansen* and Dietrich Gradmann

Max-Planck-Institut für Biochemie, Abteilung Membranbiochemie, D-8033 Martinsried, Federal Republic of Germany, and
* Institut für Angewandte Physik der Universität Kiel, Neue Universität, Haus N 61 A, D-2300 Kiel, Federal Republic of Germany

Summary. Reaction kinetic analysis of the electrical properties of the electrogenic Cl^- pump in *Acetabularia* has been extended from steady-state to nonsteady-state conditions: electrical frequency responses of the *Acetabularia* membrane have been measured over the range from 1 Hz to 10 kHz at transmembrane potential differences across the plasmalemma (V_m) between -70 and -240 mV using voltage-clamp techniques. The results are well described by an electrical equivalent circuit with three parallel limbs: a conventional membrane capacitance c_m, a steady-state conductance g_o (predominantly of the pump pathway plus a minor passive ion conductance) and a conductance g_s in series with a capacitance c_p which are peculiar to the temporal behavior of the pump. The absolute values and voltage sensitivities of these four elements have been determined: c_m of about 8 mF m^{-2} turned out to be voltage insensitive; it is considered to be normal. g_o is voltage sensitive and displays a peak of about 80 S m^{-2} around -180 mV. Voltage sensitivity of g_s could not be documented due to large scatter of g_s (around 80 S m^{-2}). c_p behaved voltage sensitive with a notch of about 20 mF m^{-2} around -180 mV, a peak of about 40 mF m^{-2} at -120 mV and vanishing at -70 mV. When these data are compared with the predictions of nonsteady-state electrical properties of charge transport systems (U.-P. Hansen, J. Tittor, D. Gradmann, 1983, *J. Membrane Biol. in press*), model "A" (redistribution of states within the reaction cycle) consistently provides magnitude and voltage sensitivity of the elements g_o, g_s and c_p of the equivalent circuit, when known kinetic parameters of the pump are used for the calculations. This analysis results in a density of pump elements in the *Acetabularia* plasmalemma of about 50 nmol m^{-2}. The dominating rate constants for the redistribution of the individual states of the pump in the electric field turn out to be in the range of 500 sec^{-1}, under normal conditions.

Key Words *Acetabularia* · electrogenic pump · electrical frequency response · membrane capacitance · voltage-dependent reaction kinetics

Introduction

The electrogenic Cl^- pump in the outer plasma membrane (plasmalemma) of the giant, unicellular marine alga *Acetabularia* has turned out to be a good system to study electrical properties of a charge-transporting enzyme which can convert metabolic energy into electric energy and *vice versa* [3, 5, 7]. By application of Eyring rate theory to cyclic reaction systems of active ion transport [8], the steady-state electrical properties of the pump as measured by its current-voltage relationships ($i_p(V_m)$) has resulted in an accurate and meaningful reaction kinetic description of the pump on a molecular level [5]. Furthermore, this analysis could provide consistent interpretations of changes in the pump as they occur upon illumination [5] or different substrate concentrations [9]. In addition, the predictions of the model on unidirectional Cl^- efflux through the pump including its dependence on the electrical potential difference across the plasmalemma (V_m) could be verified quantitatively [12].

The aim of this study is now to extend this reaction kinetic analysis of the electrical properties of the electrogenic Cl^- pump in *Acetabularia* from steady-state conditions to nonsteady-state conditions. A detailed description of the required theory is given by ref. [10].

Several properties reported from the electrogenic Cl^- pump in *Acetabularia* seemed to promise successful application of this theory to this pump:

1. The electrogenic Cl^- pump is by far the most dominant ion transport system in *Acetabularia* under normal conditions [3].

2. Extremely large exchange rates of Cl^- (up to 10^{-5} mol m^{-2} sec^{-1}) under conditions when the pump is operating [3, 13], point to either high turnover rates (in sec^{-1}) of the enzyme or to a high density N (in mol m^{-2}) of active pumps in the membrane.

3. Under normal conditions, the temporal response of V_m (in the range of a msec [6]) to

square-wave current steps, yields an unusually large membrane capacitance of about 50 mF m^{-2} [6], which is significantly larger than normal capacitance values of biological membranes (8 to 12 mF m^{-2}).

If these V_m responses and the large capacitance reflect properties of the pump, the limiting rate constants involved (k some 100 sec^{-1}) are expected to be slow enough to be detected conveniently. In this case, the high transport rates (ϕ around 10^{-5} mol m^{-2} sec^{-1}) point to an $N = \phi/k$ of around 10^{-7} mol m^{-2}.

In a recent study [16] on a related alga (*Valonia*), pulse charge experiments revealed a similar large capacitance (in addition to the normal membrane capacitance), equivalent to a density of 0.5×10^{-7} mol m^{-2} of mobile charges in the membrane, which redistribute in the electric field with a rate constant around 500 sec^{-1}. In our study, very similar properties are found for *Acetabularia* which, however, can be identified as intrinsic features of the electrogenic pump.

There are several, mathematically equivalent methods to obtain the desired quantitative data of the temporal behavior of a system by recording its response in time upon small perturbations. Relaxation analysis of the responses upon pulse- or step-functions as perturbing stimuli is applied to biological systems traditionally. On the other hand, frequency response analysis on sinusoidally modulated signals is more sensitive and, therefore, increasingly used also by biologists. When electrical stimuli and responses are under investigation, this system-analytical approach is called "AC impedance analysis". In this study, voltage-clamp techniques were used to apply AC impedance analysis to the plasmalemma of *Acetabularia* with particular respect to different steady-state membrane potential V_m.

Parts of this study have briefly been reported recently [15].

Materials and Methods

Material

Cells of *Acetabularia mediterranea* were cultured as usual [11]. At least 7 days before an experiment, young, cylindrical cells (*ca.* 30 mm in length and 0.3 mm in diameter) which had not yet developed a cap, were transferred to artificial seawater (in mM: 461 Na^+, 10 K^+, 53 Mg^{++}, 10 Ca^{++}, 529 Cl^-, 28 SO_4^{2-}, 2 HCO_3^-, 10 Tris/HCl buffer, pH 8) for equilibration. This medium was also used for the experiments.

In order to eliminate undesired cable problems for the electrical analysis, short (1 to 3 mm) segments were tied off by two ligatures from the cylindrical stalk of the cells. Thus, electrophysiologically "spherical" segments were used with a length shorter than the cable length (> 1.6 mm [3]) when the segments are punctured in the middle. Therefore, approximately uniform current densities could be expected over the entire membrane area of these preparations. Eventual radial or longitudinal inhomogeneities have been ignored. In order to ensure proper ligatures, the two remaining ends beyond the ligatures were killed (by cutting off), and only those segments were used which displayed a proper resting potential, V_r. A comparison of membrane currents from these and previous preparations [3, 6] results in coincidence within statistical limits.

Experimental Setup

Conventional glass microelectrode techniques with two intracellular electrodes have been applied. The electrical circuit diagram including the voltage-clamp circuit has been described in detail previously [2]. Some modifications enabled measurements up to 10 kHz: low resistance (1 to 2 MΩ) electrodes have been used, pulled with a David Kopff vertical pipette puller (Mod. 700 C), and filled with saturated KCl solution. The capacitance of the input circuit has been minimized to about 20 pF by positioning the preamplifier immediately (< 80 mm) behind the electrode tip. Using negative capacitance feedback, the temporal resolution of the voltage recording system has been improved in addition.

For measurements at high frequencies, when the voltage-clamp circuit was too slow to follow the sinusoidal voltage-clamp command with full voltage amplitude, the amplitude of the command voltage was adjusted to obtain actual voltage amplitudes ΔV_m between 2 and 8 mV across the membrane. It can be shown that under these and ideal clamp conditions, the amplitude and phase relationships of the investigated system are recorded correctly (theoretical considerations and measurements on "dummy" cells). Measurements at high frequencies were limited to about 10 kHz, when the capacitive shunt between the current-injecting electrode and the voltage-recording electrode started to short circuit the high resistance electrode tips and the membrane under investigation. Such a shunt at high frequencies causes an apparent increase of the impedance, which marked the upper limit of valid measurements.

Measuring Procedure

The spheres were transferred to an open perspex dish (*ca.* 1 ml volume with connections for external current electrode, reference electrode for voltage recording, inlet and outlet for medium) on a microscope (Leitz, Labolux 2, magnification: 3.5 × 16). In the empty but wet dish, the spheres adhered tightly enough to the bottom, thus enabling convenient puncturing with two microelectrodes. Touching the spheres outside with the voltage-recording electrode tip yielded the reference point for intracellular voltage recordings. Control determinations of the reference point in the open medium after a measurement yielded good coincidence. Deviations by more than 10 mV have not been tolerated.

When the two electrodes for voltage recording and current injection, respectively, were impaled, guided in an

angle of about 45° by two (Leitz) micromanipulators, a steady stream of fresh medium (*ca.* 100 µl sec^{-1}) was fed through the experimental chamber. Despite apparently good impalements, initial voltage recordings were usually very low. When the membrane potential V_m eventually recovered to the resting potential V_r in these preparations, the same characteristic shoulder around the equilibrium potential of K^+ (E_K about −90 mV) as in normal cells [2] was observed. During this recovery, the length and diameter of the preparation was measured microscopically for determination of the surface area.

When V_r was acceptable (stable and more negative than −150 mV, - normally V_r around −170 mV, inside negative), V_m was clamped first by a step command to a desired steady-state level. When, after the very slow response in the range of some 10 sec [2], the clamp current I had reached a stable value, a small sinusoidal clamp command was superimposed on the step command. Pen chart recordings (DC, direct current) of V_m and I have been taken continuously. The sinusoidal changes in V_m (ΔV_m) and the corresponding clamp current ΔI for each V_m step have been recorded for about four cycles by a dual digital oscilloscope and stored by a "floppy" disc unit (Nicolet, Explorer III, Model 204-A, 8 bit).

In addition to those time constants which are under investigation in this article, time constants in the range of 1 to 10 sec are known to occur in the electrical response of the *Acetabularia* membrane [2, 3, 4, 6]. The underlying processes of these slow events can only indirectly be related (regulation?) to the ion transport mechanisms, and may virtually be ignored in this study. Therefore, the lower frequency limit of 1 Hz was chosen. High frequency measurements were limited to about 10 kHz by the apparatus. The frequency intervals were chosen between 2 and 9 points per decade with increasing resolution for higher frequencies (compare Figs. 4 and 5). Recordings of one frequency response from 1 Hz to 10 kHz took about 10 min. During this period, stability of the membrane is required. Stability has been monitored by the steady-state recordings of the clamp current on the pen chart recorder.

Evaluation

Amplitude ratios, $\Delta V_m/\Delta i_m = |\vec{R}|$, between the sinusoidal changes (peak to peak) in ΔV_m and the clamp current Δi_m (related to membrane surface area) as well as the phase differences $\Delta\varphi$ for each frequency f, steady-state V_m and preparation were read from replays of the data stored on floppy disc on the digital oscilloscope (compare Fig. 2). Sets of $|\vec{R}|(f)$ and $\Delta\varphi(f)$ from each V_m and cell were entered into a computer (PDP 10) to be fitted to a given transfer function by a routine according to [14]. The desired parameters have been obtained by the algebraic relationships given below.

For statistical representation of the results, geometric means and errors, exp(SEM of ln(x)), are used, yielding somewhat smaller means than arithmetic ones and asymmetric error bars (errors are now given as factors by which the means are divided and multiplied in order to describe the confidence interval). This statistical treatment is legitimate and more appropriate for large scatter.

Definitions

In this section, some formal relationships are briefly introduced which will be used for the presentation and discussion of the results. Explicit derivations of the expressions are given in refs. [8] and [10].

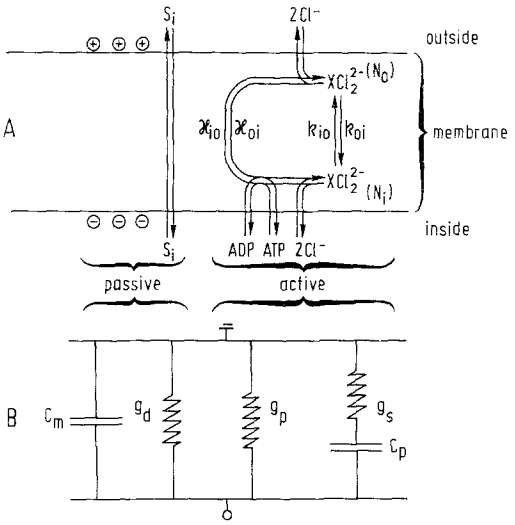

Fig. 1. Reaction kinetic model (*A*) and equivalent circuit (*B*) of a membrane with an electrogenic pump in parallel with passive ion diffusion. Reaction scheme of active transport represents the electrogenic Cl^- pump in *Acetabularia* according to refs. [7] and [12]. For derivation of equivalent circuit of pump, *see* ref. [10]. Symbols are explained in Definitions

Starting from an explicit reaction scheme of the electrogenic Cl^- pump [12], it can be shown [8] that a correct description of its steady-state current-voltage relationship, $i_p(V_m)$, can be achieved by a reduced reaction kinetic model (Fig. 1*A*, right) consisting of an enzyme 'X' with the density N (in mol m^{-2}), distributed in one representative state outside and another one inside with the densities N_o and N_i, respectively:

$$N = N_i + N_o. \tag{1}$$

The transition of charge is described by one pair of voltage-sensitive rate constants

$$k_{io} = k_{io}^o \exp(zu/2) \quad \text{and} \quad k_{oi} = k_{oi}^o \exp(-zu/2) \tag{2a, b}$$

where the superscript 'o' denotes the values of the rate constants (in sec^{-1}) at zero V_m,

$$u = V_m F/RT \tag{3}$$

is the normalized membrane potential, z is the charge number (−2 in our case) and the factor 2 in the denominator of the exponents in Eqs. (2a) and (2b) account for the assumption that the potential peak for the transition of charge is located in the middle of the membrane thickness. The latter assumption has been justified as

a first approach to the electrical properties of the electrogenic pump in *Acetabularia* [7].

The voltage-insensitive part of the reaction scheme can be summarized by two voltage-insensitive gross rate constants κ_{io} and κ_{oi}. These two constants formally describe association and dissociation of substrates as well as the recycling of the molecule X without Cl^-.

The left part of Fig. 1*A* simply represents the passive electrical properties of the membrane, indicated by passive ion conductance of various charged substances S_i and the charges on the lipid-water interfaces for normal membranes (inside negative).

It can now be shown that the electrical behavior of such a membrane with passive properties and an active ion transport system in parallel, can be described by an equivalent circuit as depicted in part *B* of Fig. 1.

c_m is the membrane capacitance, normally pretty close to 10 mF m^{-2} for biological and artificial lipid membranes.

g_d is the membrane conductance due to passive ion diffusion and maybe other charge-carrying processes which are not of particular interest. For *Acetabularia*, g_d has been determined to 0.28 S m^{-2} for V_m more negative than E_K [3]; for V_m more positive than E_K, g_d becomes larger (up to 6 S m^{-2}) [2].

g_p is the steady-state slope conductance of the electrogenic pump which depends on V_m (*see below*). For normal conditions, g_p is at least one order of magnitude larger than g_d [3] and g_d can, therefore, virtually be ignored in this study. This approach leads to

$$g_o = g_p + g_d \approx g_p. \tag{4}$$

The physical meaning of c_p can crudely be imagined by the density of charged states of the pump within the membrane, and g_o and g_s by their mobility for redistribution in the electric field. However, the exact meaning of c_p, g_o and g_s in reaction kinetic terms is given by the following relationships according to [10]:

$$g_o = N \frac{z^2 F^2}{2RT} \cdot \frac{(k_{oi}(k_{io}+\kappa_{io}) + k_{io}(k_{oi}+\kappa_{oi}))(\kappa_{io}+\kappa_{oi})}{K^2} \tag{5}$$

with

$$K = k_{io} + k_{oi} + \kappa_{io} + \kappa_{oi} \tag{6}$$

$$c_p = \frac{g_o}{K} \frac{k_{oi}+k_{io}}{\kappa_{oi}+\kappa_{io}} \tag{7}$$

and

$$g_s = c_p K. \tag{8}$$

For the description and analysis of the primary results (Bode plots, examples in Figs. 4 and 5), the following transfer function is used:

$$\vec{R} = \text{const} \cdot \frac{1+p\tau_n}{1+p(\tau_1+\tau_2)+p^2\tau_1\tau_2} = \text{const} \cdot \frac{1+p\tau_n}{(1+p\tau_1)(1+p\tau_2)} \tag{9a, b}$$

where $\vec{R} = |\vec{R}| \exp(\varphi\sqrt{-1})$ is the complex impedance describing both, magnitude $|\vec{R}|$ and phase angle $\varphi = \arctan(\mathrm{Im}\vec{R}/\mathrm{Re}\vec{R})$ and $p = 2\pi f\sqrt{-1}$ with f being the frequency in Hz. This transfer function (Eq. 9) has three characteristic frequencies: one "zero" and two "poles." The zero is given by the numerator for $p = -1/\tau_n$, when $\vec{R}$ becomes zero and the two poles are given by the denominator for $p = -1/\tau_1$ and $p = -1/\tau_2$, when $\vec{R}$ becomes infinity.

The numerical values of the four parameters const, $\tau_n = 1/K$, $(\tau_1+\tau_2)$ and $\tau_1\tau_2$ result from the fits. These four values are used to calculate the desired four values of g_o, c_m, c_p and g_s of the equivalent circuit subsequently:

$$g_o = 1/\text{const} \tag{10}$$

$$c_m = g_o \tau_1 \tau_2 / \tau_n \tag{11}$$

$$c_p = g_o(\tau_1+\tau_2-\tau_n-\tau_1\tau_2/\tau_n) \tag{12}$$

$$g_s = c_p/\tau_n. \tag{13}$$

Results

Figure 2 illustrates the determination of amplitudes (ΔV_m, ΔI) and phase differences ($\Delta\varphi$) by means of an example of tracings of a pair of sinusoidal changes in V_m and I under voltage-clamp conditions as recorded from the oscilloscope. Steady-state V_m and current (DC-V_m and DC-I) are taken from the chart recordings before and after the sine-wave command was superimposed on the steady-state clamp voltage. The recordings of DC-I were only used here as a check for stable membrane conditions and did not enter the calculations.

Since proportionality between ΔI and ΔV_m is absolutely essential for the significance of the

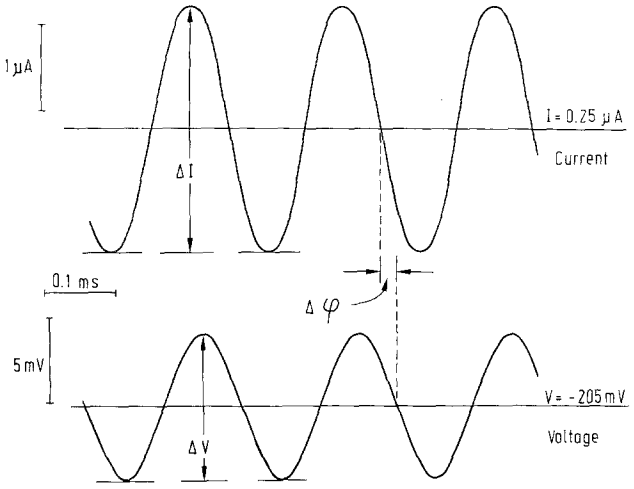

Fig. 2. Example of sinusoidal time course of current and voltage changes under experimental conditions (voltage clamp). Illustration of the parameters ΔI, ΔV_m, $\Delta\varphi$ and V_m, which are evaluated for further data processing

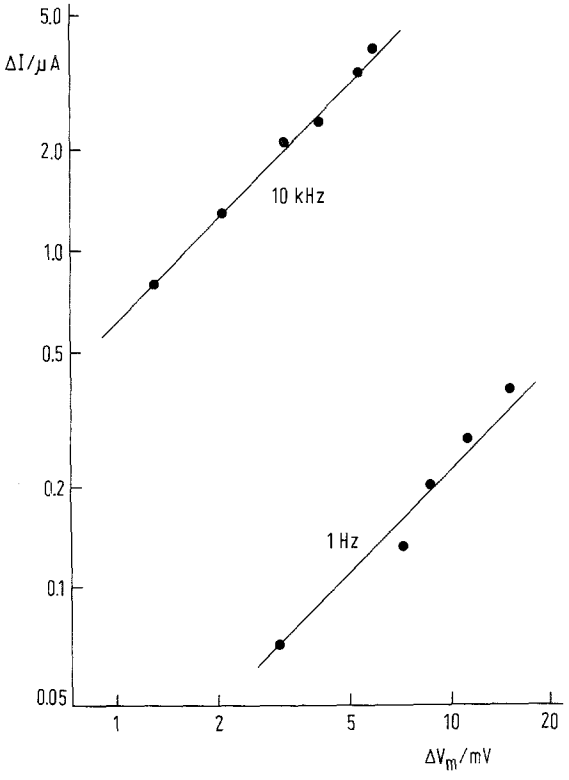

Fig. 3. Examination for linearity of $\Delta V_m/\Delta I$ at lowest (1 Hz) and highest (10 kHz) frequency used. Steady-state V_m clamped at -138 mV, where large nonlinearities are expected. Double logarithmic plot; lines have the theoretical slope of 1

final results after computation, the amplitudes have to be chosen small enough to guarantee this proportionality. Proper sinusoidal changes as in Fig. 2 indicate the required linearity. In addition, linearity has been tested systematically. Since eventual voltage-sensitive elements may cause nonlinearities depending on their associated capacitances, the test for linearity has been performed at minimum (1 Hz) and maximum (10 kHz) frequency. Furthermore, this test is most critical in a voltage range where nonlinearities are expected. From previous investigations [3] it is known that the electrogenic pump in *Acetabularia* is most sensitive to V_m in the wider range around -140 mV. Therefore, the test for linearity at a clamp voltage of -138 mV as shown in Fig. 3 is expected to be significant for the entire voltage range under investigation, as far as the electrogenic pump is concerned. According to the results in Fig. 3, linearity is guaranteed for ΔV_m smaller than 8 mV. This limit has never been exceeded for the following experiments.

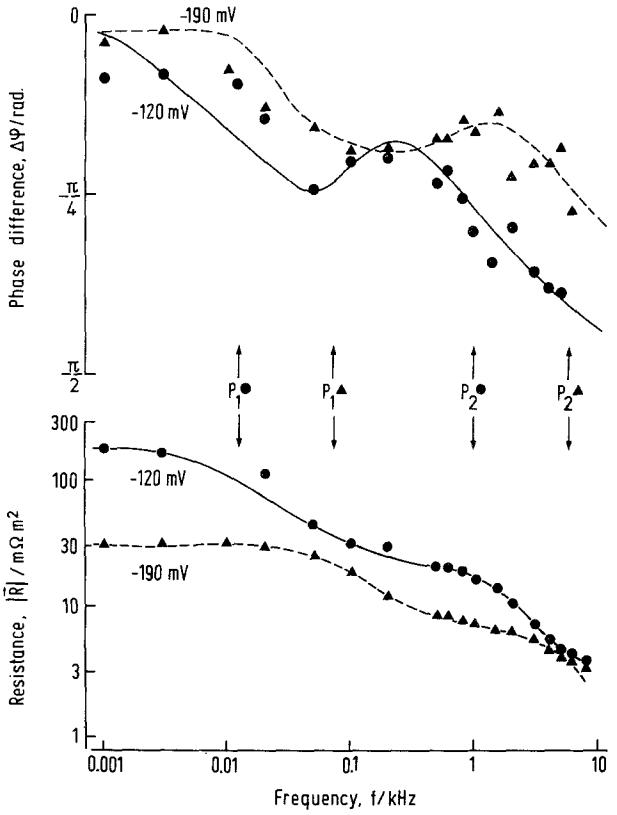

Fig. 4. Examples of Bode plots of two electrical frequency responses at $V_m = -190$ and $V_m = -120$ mV. Data from one cell segment (150782). Points are measured, lines are fits by Eq. (9). Arrows indicate location of poles: $p_{1,2} = 1/2\pi\tau_{1,2}$

Figure 4 shows two Bode plots of $|\vec{R}|$ for two V_m values (-120 and -190 mV) from one preparation. The combination of the measured values (points in Fig. 4) $|\vec{R}|(f)$ and $\Delta\varphi(f)$ represent one set of data for each V_m. Such sets of data have been fitted to Eq. (9). The computer

fits of the two examples are given in Fig. 4 by the smooth lines. Several interpretations can readily be made by inspection of those curves:

1. The number of time constants involved is 2. Fits with only one τ were much worse in general. Exceptions will be discussed separately. Hints for additional time constants may be seen, for instance, by the deviation of both measured values ($|\vec{R}|$ and $\Delta\varphi$) from the fitted curve at 20 Hz in the two -120 mV curves. The general scatter in the measurements is, however, too large for making definitive statements at present.

2. The processes associated to the two time constants are arranged in parallel. In the case of serial arrangement, the slope at the high frequency end of the $|\vec{R}|$ spectrum would approach -2 in this double logarithmic plot (Bode plot) with equal scaling in both axes. In our measurements, significant slopes steeper than -1 have never been observed. Similarly, in the $\Delta\varphi$ spectrum, $\Delta\varphi$ never significantly exceeds $-\pi/2$ in our experiments, whereas a limit of $-\pi$ is expected for serial arrangement of the processes associated with the two time constants.

3. There are no traces of an inductivity, because positive $\Delta\varphi$ values have never been observed.

4. For -190 mV, the events are faster than for -120 mV. This can be seen by the shift of the curve characteristics towards high frequency of the -190 mV curves ($|\vec{R}|$ and $\Delta\varphi$) compared to the -120 mV curves.

5. The "DC resistance" as given by the $|\vec{R}|$ values at the low frequency end, is lower at -190 mV compared to -120 mV.

While Nos. 4 and 5 confirm previous investigations [3, 4], Nos. 1 to 3 are peculiar to this study. These points show that the used transfer function with one zero and two poles (Eq. 9) and the equivalent circuit (Fig. 1*B*) are appropriate. On the other hand, for a $V_m = -70$ mV, the description with just one pole is sufficient. Figure 5 shows an example Bode plot for this situation.

From the parameters of the fitted transfer functions, the desired values for g_o, g_s, c_p and c_m are obtained by Eqs. (10) to (13). The individual results of these parameters from each set of data are listed in Table 1 in the order of increasing (negative) V_m. Lines with the same identification No. (date of experiment) indicate measurements from the same preparation. The small numbers of observations at high negative

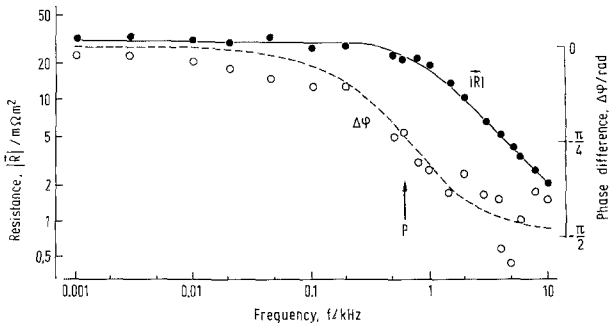

Fig. 5. Example of Bode plot of electrical frequency response at $V_m = -70$ mV (150782). Points are measured, lines are fitted to transfer function with one pole only. Arrow indicates pole: $p = 1/2\pi\tau$

V_m are due to instabilities of the membranes in this V_m range. Similarly, the recordings at -70 mV represent large deviations from V_r, which often causes instabilities during the 10-min period required for an entire set of data.

The same data as in Table 1 are plotted in Figs. 6 and 7 as (geometric) means and errors. Figure 6 gives the conductance values (g_o: part *A* and g_s: part *B*) plotted versus V_m. The absolute values and the voltage-sensitivity of g_o agree with the bell-shaped "early conductance" characteristics of previous studies [3, 6], when the temporal resolution did not allow the distinction of the two time constants of the system (Fig. 1). This agreement must be expected, since g_o and "early conductance" are virtually synonymous - only g_o is measured by sinewaves and the "early conductance" was measured by square-wave currents. The peak conductance of g_o is not intrinsically located at the equilibrium potential of the pump ($E_p = -190$ mV, [3, 6]) but usually occurs in its close (± 20 mV) neighborhood (about -175 mV in these experiments).

As for g_s (Fig. 6*B*), the statistical deviations turned out to be rather large. Therefore, a correlation of g_s with V_m could not be identified by these measurements. The small g_s value at -240 mV is singular and, therefore, statistically insignificant.

The g_s and c_p values at -70 mV need extra comment. The frequency responses at -70 mV could be fitted without loss of accuracy by a transfer function with just one time constant (one pole only). Thus the limb of the equivalent circuit consisting of g_s and c_p (compare Fig. 1*B*) does not show up. The experimental results offer two explanations: g_s has become very small or c_p has become very small. Model *A* in ref. [10] predicts increasing values for g_s at more

Table 1. Values of g_o, g_s, c_p and c_m as they result by fitting individual frequency responses from different V_m to Eq. (9) and comparison with equivalent circuit Fig. 1*B*[a]

V_m/ (mV)	ID No./ (date)	g_o/ (S m^{-2})	g_s/ (S m^{-2})	c_p/ (mF m^{-2})	c_m/ (mF m^{-2})
−70	070782	13.0	–	<8.0	11.6
	150782	31.8	–	<8.0	7.6
−120	310382	17.9	166.7	67.5	12.5
	180682	22.8	333.3	26.4	7.1
	060782	18.6	108.5	46.0	11.6
	150782	5.5	29.8	55.8	6.4
	180782	78.7	40.5	33.6	26.2
−140	250382	34.7	49.5	87.3	6.0
	310382	42.0	75.2	15.7	4.2
	290482	18.9	75.2	29.3	9.4
	030582	196.1	103.1	18.1	5.3
	050582	131.6	90.1	14.9	4.8
	100582	60.2	76.3	33.3	10.5
	180682	67.6	128.2	46.3	13.0
	150782	19.3	70.9	47.8	5.2
−160	250382	103.1	85.5	34.9	7.1
	310382	100.0	53.2	12.7	2.7
	030582	238.1	285.7	15.1	9.5
	050582	44.1	61.3	42.5	8.3
	100582	142.9	106.4	10.4	9.5
	290682	30.2	55.9	31.6	10.6
	150782	27.1	92.6	56.2	5.8
−180	250382	120.5	43.9	8.0	5.0
	310382	96.2	48.3	10.5	2.2
	030582	227.3	434.8	12.7	14.3
	100582	71.9	196.1	63.1	9.2
	290682	25.4	56.8	24.5	10.0
−190	250382	100.0	70.4	48.0	7.1
	250382′	58.5	55.9	29.7	6.5
	150782	30.7	93.5	49.5	6.0
	180782	43.9	105.3	32.1	11.9
	210782	86.2	86.2	22.1	11.8
−205	290682	23.3	48.5	47.7	11.1
	180782	58.5	156.3	26.0	6.6
−240	290682	21.2	18.9	27.2	13.9

[a] Values for $V_m = -70$ mV: fitted to transfer function with one pole only (g_o and c_m in parallel), c_p here smaller than general scatter (SD) in c_m (8.0 mF m^{-2}); explicit discussion in text.

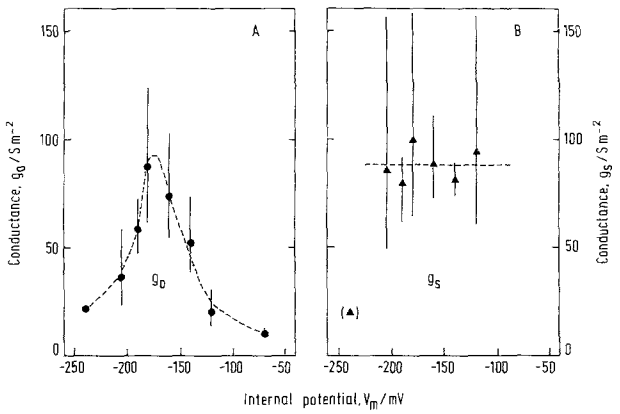

Fig. 6. Average results of membrane conductance g_o(*A*) and g_s(*B*) as function of clamped V_m. Data from Table 1. g_o and g_s are defined by Eqs. (4), (5) and (8), respectively, and Fig. 1*B*. The lines are drawn to guide the eye

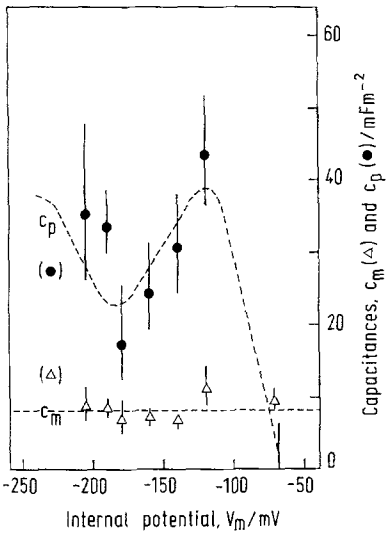

Fig. 7. Average results of membrane capacitance c_m and c_p as function of clamped V_m. Data from Table 1. c_m and c_p are defined by Fig. 1*B*, c_p by Eq. (7) as well. c_p at −70 mV: smaller than scatter in c_m (8.0 mF m^{-2}). The lines are drawn to guide the eye

positive potentials. Thus the interpretation that c_p and not g_s vanishes, satisfies both theory and experimental data. There is an alternative situation which also leads to a transfer function with a single time constant: g_s becomes very large, thus merging c_p with c_m into one capacitance. However, the experimental data assign to this capacitance the same value as to c_m alone, leading to the same conclusion as above: c_p is zero within the experimental scatter. This situation is illustrated in Fig. 7 by presenting only an error bar and no (average) point for the c_p value at −70 mV. Thus, for −70 mV, a small c_p value is shown in Table 1 and Fig. 7, whereas g_s is omitted, as small c_p renders g_s immeasurable.

The resulting two capacitance values of c_m and c_p are plotted in Fig. 7 versus V_m. The membrane capacitance c_m turned out to be virtually voltage insensitive and close to the value of 10 mF m^{-2} which is considered to be characteristic for biological membranes. In contrast, c_p displays - despite its scatter - a minimum at −180 mV. Statistical comparison of the values at −180 mV with those from −120 mV (*t*-test) yield a nominal significance level of $P = 0.023$. If

the -180 mV values are compared with the -190 mV values, the t-test yields $P=0.087$. From these comparisons, the notch of the c_p values at -180 mV can be considered significant. The singular value of c_p at -240 mV cannot be used for statistical purpose. However, the small values at -70 mV are very important as described above.

The large scatter of the data may be due to the fact that individual variations of particular rate constants can add up to large deviations of the resulting electrical parameters which are measured. In order to reduce the large scatter, several legitimate, statistical manipulations were carried out, in particular in search for factors, such as g_o, g_d, age and size of cells, which might correlate with the scatter. Since no such correlation could yet be detected, the data must be taken as they are at the present, which is perfectly sufficient to justify the main conclusions reached.

Discussion

The present investigation reveals the biophysical background of a strange experimental result: whereas nearly all biological and artificial membranes display a membrane capacitance close to 10 mF m^{-2}, a value of 50 mF m^{-2} was found in *Acetabularia* [3, 6]. This large value could not be explained by invaginations of the plasmalemma, as those have never been documented to exist in *Acetabularia*.

The higher resolution of the wide-band frequency response analysis of membrane impedance leads to the refined equivalent circuit which includes the limb consisting of c_p and g_s (Fig. 1*B*). In those previous investigations [3, 6], c_m and c_p were merged into one capacitor. The detection of g_s enables the assignment of the two capacitors to two different biological functions. c_m is the usual membrane capacitance with a value of about 10 mF m^{-2}. c_p is associated with the nonsteady-state behavior of the predominant ion transport system in *Acetabularia*. There are two alternative possibilities for a biophysical interpretation of c_p according to ref. [10].

Model A: A high density of charge-transporting elements is present in the *Acetabularia* plasmalemma. This conceptually simpler model is discussed below in more detail.

Model B: A predominant, charge-carrying, cyclic reaction system in the membrane equilibrates with an inactive, "lazy" state. The time constant of the equilibration can be arbitrarily small, thus causing apparently slow changes in the electrical response of the charge-carrying cycle itself, which can be very fast (for details of this model B, *see* ref. [10]). An intrinsic feature of this model is the possibility of apparent inductivities; in our case, the slow response would be expected to switch its sign (capacitive to inductive behavior) for V_m more negative than E_p, vanishing in amplitude while passing E_p. This behavior, however, could never be documented during this study. Therefore, this possibility must be excluded to explain the phenomenon of large c_p values in *Acetabularia*.

It should be mentioned, however, in this context that for the "late" response (range some 1 to 10 sec), such apparent inductivities can be observed in *Acetabularia*, under conditions when the membrane is hyperpolarized beyond E_p, i.e. the time course of the clamp current upon large, hyperpolarizing V_m steps, regularly displays a sigmoid increase to a stable value in some 10 sec after the initial, fast response (D. Gradmann, A. Schafmeister and J. Tittor, *unpublished results*).

Since model B must be rejected for our present purpose, the alternative model A should be examined in more detail, in particular with respect to the biophysical nature of c_p. The electrogenic Cl^- pump is the most dominant ion transport system in the *Acetabularia* plasmalemma membrane. Therefore, the first guess is that the electrogenic pump might be responsible for the apparent c_p. This hypothesis can quantitatively be examined on the basis of the theory of the impedance of an active ion transport system [10] and previous reaction kinetic analysis of $i_p(V_m)$ [5, 7, 12].

The comparison of the experimental data and the predictions of model A can be tested by computer fitting routines or directly. For the direct approach, we can choose $V_m=E_p=-190$ mV, where k_{io} and k_{oi} can be considered to be identical ($=k'$). Equation (5) then simplifies to

$$g_o=N\frac{z^2F^2}{2RT}\frac{k'(\kappa_{io}+\kappa_{oi})}{K}. \tag{14}$$

Furthermore, the relationship

$$q=\frac{g_o}{g_s}=\frac{\kappa_{io}+\kappa_{oi}}{k_{io}+k_{oi}}, \tag{15}$$

derived from Eqs. (7) and (8), is used.

Table 2. Model parameters (for definitions *see* Fig. 1*A*)

	$V_m=E_p$	$V_m=0$
k_{io} (sec^{-1})	250	0.125
k_{oi} (sec^{-1})	250	500000
κ_{io} (sec^{-1})	500	500
κ_{oi} (sec^{-1})	500	500

$N=60$ nmol m^{-2}; $z=-2$; $E_p=-190$ mV.

The values of the zeros at -190 mV, $\tau_n=1/K$, can be read from Table 1 using Eq. (8). This yields an average $K=2{,}317\,sec^{-1}$ at -190 mV. The average ratios of q can also be obtained from Table 1, yielding a value of 0.727 at -190 mV. From these numbers, $k'=671\,sec^{-1}$ and $\kappa_{io}+\kappa_{oi}=975\,sec^{-1}$ are obtained. Rewriting of Eq. (14) now yields a value for $N=27$ nmol m^{-2} with average $g_o=58.4$ S m^{-2} from Table 1.

The knowledge of $\kappa_{io}+\kappa_{oi}$ of about $1{,}000\,sec^{-1}$ enables another direct estimate of N by the two saturating currents for large positive (i_{s+}) and large negative (i_{s-}) V_m displacements:

$$i_{s+}-i_{s-}=N|z|F(\kappa_{io}+\kappa_{oi}). \tag{16}$$

Using data from ref. [7] ($i_{s+}\approx\approx -i_{s-}\approx 6$ A m^{-2}) results in an N of about 60 nmol m^{-2}. Since symmetrical saturation currents as found for $i_p(V_m)$ in *Acetabularia* [5, 7], are equivalent to identical κ values, we obtain $\kappa_{io}=\kappa_{oi}=500\,sec^{-1}$ as representative values. The direct determination of the k values above suffers from the unreliable g_s values. In order to approximate the shape of the $c_p(V_m)$ curve (Fig. 7), k' has empirically been determined to $250\,sec^{-1}$. This choice is justified within the statistical limits. The complete list of the kinetic 2-state parameters is now given in Table 2. The figures in Table 2 are valid for the following, approximate substrate concentrations *in situ:* $[Cl^-]_o=500$ mM, $[Cl^-]_i=500$ mM, $[ATP]_i=1$ mM, $[ADP]_i=0.1$ mM, $[P_i]_i=10$ mM. Using these numbers from Table 2 yields quantitative predictions about the V_m sensitivity of the elements g_o, g_s and c_p according to Eqs. (2), (4), (7) and (8). These predicted relationships are illustrated in Figs. 8 and 9.

For g_o, the typical bell-shape with a peak of about 80 S m^{-2} in the neighborhood of E_p agrees well with the experimental curve (Fig. 6*A*). For g_s, a clear minimum is predicted at E_p which, however, could not be detected in the measurements (Fig. 6*B*), probably due to the large scatter. It has been described above, why

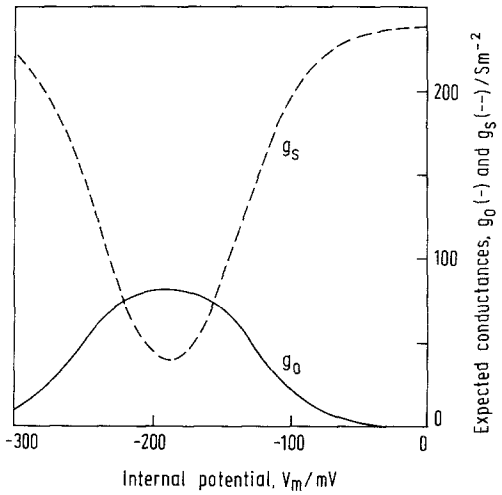

Fig. 8. Expected V_m sensitivity of g_o and g_s according to Eqs. (2), (5) (g_o) and (8) (g_s), with parameters from Table 2

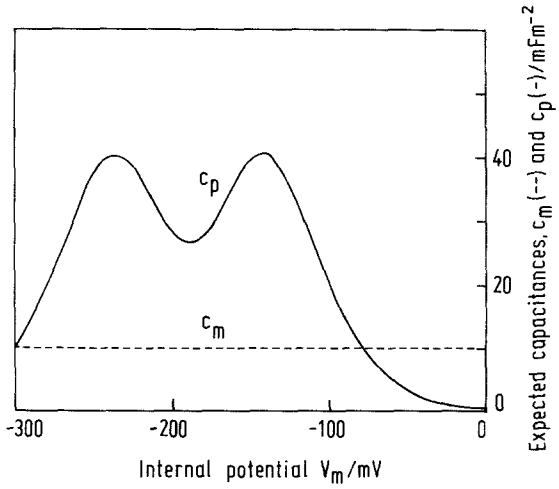

Fig. 9. Expected V_m sensitivity of c_p according to Eqs. (2) and (7), with parameters from Table 2. c_m: expectation for usual, V_m insensitive membrane capacitance

the values at -240 and -70 mV in Fig. 6*B* cannot be regarded as significant. Therefore, only the range of the absolute values (around 80 S m^{-2}) can be considered to agree between measurements and predictions.

The most characteristic curve is the V_m sensitivity of c_p (Fig. 9) with a minimum at E_p between two peaks and sharp drops for larger V_m displacements from E_p. These characteristics are nicely paralleled by the measurements (Fig. 7).

The general consistency between the predicted characteristics of g_o, g_s and especially c_p with the measured ones, favors the conclusion that the apparent capacity c_p is due to the electrogenic pump and that this pump populates the plasmalemma with the high density

of 60 nmol m^{-2}. Compared with the 27 nmol m^{-2} as obtained above by an alternative calculation, roughly 50 nmol m^{-2} can be considered as a fair estimate for the density of pump molecules in the *Acetabularia* plasmalemma.

It should be noted that the measured peak in g_o (Fig. 6*A*) is sharper than in the theoretical example (Fig. 8). This discrepancy could be avoided by choosing somewhat larger k values. However, by this assumption, in turn, the two peaks in c_p (Fig. 9) would merge into one single peak at E_p. By inspection of the data (Fig. 7), this possibility (which cannot alter the main conclusion) is very unlikely but cannot be ruled out by rigorous statistical means. Furthermore, the theoretical c_p curve (Fig. 9) is displaced by about -20 mV from the measured characteristics (Fig. 7). Whether these deviations between theory and measurements are due to experimental or theoretical errors, or whether they indicate the effect of still unresolved processes, these are still open questions which are considered to be of secondary importance at present, especially since the scatter of the present data does not justify any further refinement of the model.

The mentioned results from *Valonia* [16] appear to be virtually identical with our (independent) findings. However, since the measurements in *Valonia* have been carried out between the vacuole and outside, the observed effects could not be localized there to occur in a particular membrane (tonoplast or plasmalemma). As for *Acetabularia*, the electrode tips have been reported to be located in the cytoplasmic compartment [1, 6], which is strongly supported by our measured c_m values around 10 mF m^{-2} (measuring two membranes in series, an apparent capacity of 5 mF m^{-2} would be expected, if each membrane behaves typically) and by $|\vec{R}|(f)$ and $\Delta\varphi(f)$ characteristics at high frequencies, as discussed above. Therefore, the effects described in *Acetabularia* can clearly be attributed to the plasmalemma, in which the electrogenic pump has been demonstrated to be located [1].

Despite the similar environmental conditions of *Valonia* and *Acetabularia*, as well as their close taxonomic relationship (*Chlorosiphonales*), the apparent agreement of the results may point to the same physiological entity. However, for *Valonia* a pH-sensitive mechanism of turgor-pressure sensing has been suggested, because the large capacitance in *Valonia* (V_m sensitivity not reported) correlates with external pH and turgor pressure [16], whereas the evidence presented here on *Acetabularia* apparently identifies the large capacitance as an intrinsic property of the electrogenic Cl^- pump.

Conclusions

1. The extension of the reaction kinetics of active ion transport from steady-state [8] to non-steady-state conditions [10] provides a satisfying description of the electrogenic Cl^- pump in *Acetabularia*.

2. This pump populates the plasmalemma of *Acetabularia* with a density of about 50 nmol m^{-2}.

3. This high density of pump molecules causes an apparent voltage-sensitive capacitance of about 30 mF m^{-2} under normal conditions.

4. Under normal conditions, the effective rate constants for redistribution of different (charged) states of the pump in the electric field are in the range of 500 sec^{-1}.

This work was supported by grants of the Deutsche Forschungsgemeinschaft (Gr 409/7, 8, 9 and Ha 712/7-2). For computations, the PDP 10 of the computer center of the University of Kiel and the VAX 3.0 of the Max-Planck-Institute for Biochemistry in Martinsried were used. We thank Prof. Dr. D. Oesterhelt for generous support in his laboratories.

References

1. Freudling, C., Gradmann, D. 1979. Cable properties and compartmentation in *Acetabularia*. *Biochim. Biophys. Acta* **552**:358–365
2. Gradmann, D. 1970. Einfluss von Licht, Temperatur und Aussenmedium auf das elektrische Verhalten von *Acetabularia*. *Planta* **93**:323–353
3. Gradmann, D. 1975. Analog circuit of the *Acetabularia* membrane. *J. Membrane Biol.* **25**:183–208
4. Gradmann, D. 1976. "Metabolic" action potentials in *Acetabularia*. *J. Membrane Biol.* **29**:23–45
5. Gradmann, D., Hansen, U.-P., Slayman, C.L. 1982. Reaction kinetic analysis of current-voltage relationships for electrogenic pumps in *Neurospora* and *Acetabularia*. *In:* Electrogenic Ion Pumps. C.L. Slayman, editor. (Current Topics in Membranes and Transport, Vol. 16.) pp. 257–276. Academic Press, New York
6. Gradmann, D., Klemke, W. 1974. Current-voltage relationship of the electrogenic pump in *Acetabularia mediterranea*. *In:* Membrane Transport in Plants. U. Zimmermann and J. Dainty, editors. pp. 131–138. Springer-Verlag, Berlin
7. Gradmann, D., Tittor, J., Goldfarb, V. 1982. Electrogenic Cl^- pump in *Acetabularia*. *Philos. Trans. R. Soc. London* **299**:447–457
8. Hansen, U.-P., Gradmann, D., Sanders, D., Slayman,

C.L. 1981. Interpretations of current-voltage relationships for "active" ion transport systems: I. Steady-state reaction-kinetic analysis of Class-I mechanisms. *J. Membrane Biol.* **63**:165–190

9. Hansen, U.-P., Gradmann, D., Tittor, J., Sanders, D., Slayman, C.L. 1982. Kinetic analysis of active transport: Reduction models. *In:* Plasmalemma and Tonoplast: Their Functions in the Plant Cell. D. Marmé, E. Marrè and R. Hertel, editors. (Developments in Plant Biology, Vol. 7.) pp. 77–84. Elsevier Biomedical, Amsterdam
10. Hansen, U.-P., Tittor, J., Gradmann, D. 1983. Interpretation of current-voltage relationships for "active" ion transport systems: II. Nonsteady-state reaction-kinetic analysis of Class-I mechanisms. *J. Membrane Biol.* **75**:141–169
11. Keck, K. 1964. Culturing and experimental manipulation of *Acetabularia. In:* Methods in Cell Physiology. D.M. Prescott, editor. Vol. 1, pp. 189–213. Academic Press, New York
12. Mummert, H., Hansen, U.-P., Gradmann, D. 1981. Current-voltage curve of electrogenic Cl^- pump predicts voltage-dependent Cl^- efflux in *Acetabularia. J. Membrane Biol.* **62**:139–148
13. Saddler, H.D.W. 1970. The membrane potential of *Acetabularia mediterranea. J. Gen. Physiol.* **55**:802–821
14. Strobel, H. 1968. Systemanalyse mit determinierten Testsignalen. VEB Verlag Technik, Berlin
15. Tittor, J., Hansen, U.-P., Gradmann, D., Martensen, H.J. 1982. Nonsteady-state kinetics of Class-I transport systems observed as "pump capacitance" in electrical impedance of biological membranes. *Hoppe-Seyler's Z. Physiol. Chem.* **363**:908
16. Zimmermann, U., Büchner, K.-H., Benz, R. 1982. Transport properties of mobile charges in algal membranes: Influence of pH and turgor pressure. *J. Membrane Biol.* **67**:183–197

Received 10 September 1982; revised 5 January 1983